RESEARCH ARTICLE

Title: The core root microbiome of *Spartina alterniflora* is predominated by sulfur-oxidizing and sulfate-reducing bacteria in Georgia salt marshes, USA

Authors: Rolando, Jose L.[a]; Kolton, Max[a]; Song, Tianze[a]; Kostka, J.E.[a,b,c]

Affiliation:

[a]Georgia Institute of Technology, School of Biological Sciences, Atlanta, GA 30332, USA

[b]Georgia Institute of Technology, School of Earth and Atmospheric Sciences, Atlanta, GA 30332, USA

[c]Center for Microbial Dynamics and Infection, Georgia Institute of Technology, Atlanta, GA 30332, USA

Corresponding author:

Kostka, JE. e-mail: joel.kostka@biology.gatech.edu

Abstract

Background: Salt marshes are dominated by the smooth cordgrass *Spartina alterniflora* on the US Atlantic and Gulf of Mexico coastlines. Although soil microorganisms are well known to mediate important biogeochemical cycles in salt marshes, little is known about the role of root microbiomes in supporting the health and productivity of marsh plant hosts. Leveraging *in situ* gradients in aboveground plant biomass as a natural laboratory, we investigated the relationships between *S. alterniflora* primary productivity, sediment redox potential, and the physiological ecology of bulk sediment, rhizosphere, and root microbial communities at two Georgia barrier islands over two growing seasons.

Results: A marked decrease in prokaryotic alpha diversity with high abundance and increased phylogenetic dispersion was found in the *S. alterniflora* root microbiome. Significantly higher rates of enzymatic organic matter decomposition, as well as the relative abundances of putative sulfur (S)-oxidizing, sulfate-reducing, and nitrifying prokaryotes correlated with plant productivity. Moreover, these functional guilds were overrepresented in the *S. alterniflora* rhizosphere and root core microbiomes. Core microbiome bacteria from the *Candidatus* Thiodiazotropha genus, with the metabolic potential to couple S oxidation with C and N fixation, were shown to be highly abundant in the root and rhizosphere of *S. alterniflora*.

Conclusions: The *S. alterniflora* root microbiome is dominated by highly active and competitive species taking advantage of available carbon substrates in the oxidized root zone. Two microbially-mediated mechanisms are proposed to stimulate *S. alterniflora* primary productivity: (i.) Enhanced microbial activity replenishes nutrients and terminal electron acceptors in higher biomass stands, and (ii.) coupling of chemolithotrophic S oxidation with carbon (C) and nitrogen (N) fixation by root and rhizosphere associated prokaryotes detoxify sulfide in the root zone while potentially transferring fixed C and N to the host plant.

Key words: *Spartina alterniflora*, salt marsh, rhizosphere, microbiome, root, biogeochemical cycles, sulfur oxidation, sulfate reduction

1. Background:

Salt marsh ecosystems are structured by intertidal plant communities at the land-sea interface. Salt marshes are mostly distributed outside of the tropics and comprise a global area of ~5.5 Mha, with approximately 30% of its area located in the continental USA (Mcowen et al., 2017). On the US coastlines of the Atlantic Ocean and Gulf of Mexico, salt marshes are dominated by the smooth cordgrass *Spartina alterniflora* (Mitsch and Gosselink, 1993). Salt marsh ecosystems are biogeochemical hotspots characterized by high rates of primary productivity, organic matter mineralization, and nutrient cycling (Howarth, 1984; Kostka et al., 2002a; Kirwan et al., 2009). As a consequence of their high biological activity, *S. alterniflora* dominated salt marshes provide a broad range of ecosystem services to local and global human populations (Barbier et al., 2011). Ecosystem services provided by salt marshes include estuarine water purification, coastal protection from storm surges, sediment erosion control, maintenance of fisheries, carbon sequestration, and much more (Barbier et al., 2011, Hopkinson et al., 2019).

At the local scale, bottom-up control of *S. alterniflora* primary productivity has been associated with nitrogen (N) uptake kinetics (Mendelssohn and Morris, 2000). Low sediment redox potential and high sulfide concentration have been shown to reduce *S. alterniflora*' root energy status, decreasing the plant's available energy for N uptake (Morris and Dacey, 1984; Bradley and Morris, 1990; Koch et al., 1990; Mendelssohn and McKee, 1992). Thus, naturally occurring gradients of *S. alterniflora* primary productivity are usually found as a function of the plant's distance to large tidal creeks (Valiela et al., 1978). Sediments at closer proximity to large tidal creeks are flushed more frequently; supplying oxygen, exchanging porewater nutrients, and oxidizing toxic metabolic products such as sulfide. Conversely, areas in the interior of the marsh tend to be stagnant, accumulating chemically reduced and toxic compounds in their interstitial porewater. The microbial mediation of major biogeochemical cycles along this natural gradient in aboveground *S. alterniflora* biomass has been extensively studied (Kostka et al., 2002a; Koretsky et al., 2003; Dollhopf et al., 2005; Hyun et al., 2007; Tobias and Neubauer, 2019; Murphy et al., 2020). However, the relationship between root-microbial interactions and *S. alterniflora* primary productivity has not been characterized in detail.

Biogeochemical evidence points to tightly coupled interactions between *S. alterniflora* and microbial activity in the root zone, which facilitate the rapid exchange of electron (e^-) acceptors

(O_2, NO_3, Fe^{3+}) and donors (e.g., rhizodeposits, reduced sulfur compounds). For example, reduced sulfur compounds such as pyrite store high amounts of chemically reduced energy, and their oxidation has long been hypothesized to be an important process limiting the energy flow of salt marsh ecosystems (Howarth, 1984). Part of this energy has been speculated to be used to enhance plant growth (Howarth 1984, Morris et al., 1996), similar to the well-known symbiotic relationship between invertebrates and autotrophic sulfur-oxidizing bacteria in marine ecosystems (Dubilier et al., 2008). However, the *S. alterniflora* root-associated microbiome remains largely unexplored.

Most previous studies investigating the *S. alterniflora* root microbiome focused on understanding the factors influencing the activity and taxonomic diversity of root-associated nitrogen-fixing bacteria or diazotrophs (Whiting et al., 1986; Gandy and Yoch, 1988; Lovell et al., 2000; Brown et al., 2003; Davis et al., 2011). A few reports of other functional guilds have shown that chemolithoautotrophs conserving energy through of S, Fe, and ammonium oxidation are also enriched in the *S. alterniflora* root zone when compared to bulk sediment (Thomas et al., 2014; Zheng et al., 2016; Kolton et al., 2020). A drawback of these previous studies is that the majority did not thoroughly separate the root-associated compartment from the surrounding rhizospheric sediment (e.g., Thomas et al., 2014; Zogg et al., 2018; Kolton et al., 2020). Thus, the ecology of the closely associated *S. alterniflora* root microbiome, and its interaction with the plant host still represents an important knowledge gap to be addressed. In other plants, root microbial communities have been shown to be key players in improving plant resistance to biotic and abiotic stress, outcompeting soil-borne pathogens, modulating plant development, and transferring nutrients for plant uptake (Liu et al., 2019; White et al., 2019; Zhang et al., 2020).

To gain a predictive understanding of the beneficial interactions between a host plant and its associated root microbiome, the ecology and potential physiology of its core microbiome must be investigated. A host's core microbiome is composed of microbial taxa consistently found associated with host individuals and hypothesized to perform key functions in healthy host-microbiome systems (Shade and Handelsman, 2011). The *S. alterniflora* core root microbiome has yet to be defined. Understanding of *S. alterniflora* root microbiome could pave the way to harnessing plant-microbe interactions for the adaptive management and restoration of salt marsh habitats.

Thus, this study sought to elucidate the plant-microbe interactions linked to *S. alterniflora* primary productivity over the course of 2 years at 2 sites in GA, USA. The objectives of the study were to: 1) Evaluate the taxa that constitute the *S. alterniflora* rhizosphere and root core microbiome in GA, USA 2) Characterize the potential metabolism, physiology, and ecology of the prokaryotic taxa enriched at closer proximities to *S. alterniflora* roots along primary productivity gradients. 3) Propose a mechanistic understanding of the relationship between *S. alterniflora* and its root-associated prokaryotic community.

2. Results

2.1 Primary productivity gradient

Eight transects along a *S. alterniflora* primary productivity gradient were studied in two barrier islands in the state of Georgia, USA. A total of 24 sampling points were established and sampled during the years 2018 and 2019 in the Georgia Coastal Ecosystem - Long Term Ecological Research (GCE-LTER) site 6 at Sapelo Island (Lat: 31.389° N, Long: 81.277° W), and the Saltmarsh Ecosystem Research Facility (SERF) adjacent to the Skidaway Institute of Oceanography on Skidaway Island (Lat: 31.975° N, Long: 81.030° W) (Fig. S1). *S. alterniflora* shoot height and biomass revealed a pronounced primary productivity gradient with ranges observed within sampled points from 16.5 cm to 128.4 cm, and 1.4 g m^{-2} to 1769.8 g m^{-2}, respectively. *S. alterniflora* plants were operationally classified in three phenotypes based on shoot height: short (< 50 cm), medium (50 – 80 cm) and tall (> 80 cm). Shoot biomass averaged 149.4 g m^{-2}, 307.8 g m^{-2}, and 958.7 g m^{-2} in the short, medium and tall phenotype zones, respectively. Although shoot biomass was not closely associated with changes in leaf N concentration and total inorganic N in interstitial porewater, a strong relationship with leaf $\delta^{15}N$ and sediment C:N ratio was observed (Fig. 1a, 1b, S2, S3, S4). Higher shoot biomass was also associated with zones in the marsh with elevated sediment redox potential (Eh), which was evidenced not only by direct redox measurements, but also by higher concentrations of interstitial Fe^{3+}, and NO_3^- in the zones dominated by the tall *S. alterniflora* phenotype (Fig. 1c, Fig. S3). Conversely, in zones dominated by the short and medium phenotypes, concentrations of porewater $\sum S^{2-}$ were elevated, reaching up to 1.5 mM (Fig. S3). Shoot biomass also showed a negative relationship with leaf temperature, a proxy for leaf stomatal conductance (Ramírez et al., 2016; Fig. 1d).

Rates of extracellular enzyme activity for enzymes that catalyze the catabolism of organic C, N and P compounds, showed a strong relationship to *S. alterniflora* primary production. Rates of extracellular β-glucosidase (C), chitinase (C, and N) and phosphatase (P) activity in homogenized sediment slurries were consistently higher in zones with greater *S. alterniflora* shoot biomass at both Sapelo and Skidaway Island (Fig. 2).

2.2 Microbiome diversity

Prokaryotic diversity and abundance were investigated across the *S. alterniflora* biomass gradient in three compartments: bulk sediment, rhizosphere, and root. The root compartment was recovered by sonication in an epiphyte removal buffer; thus, likely containing mostly endosphere with residual rhizoplane microbial communities (Simmons et al., 2018). A total of 32,740 unique amplicon sequence variants (ASVs) were inferred using DADA2 v.1.10 (Callahan et al., 2016). After quality filtering, 10,068,980 high quality SSU rRNA sequence reads with a median depth of 49,619 reads per sample were used for microbiome analysis (further details in Materials and Methods). Prokaryotic communities associated with the tall *S. alterniflora* bulk and rhizosphere sediment were more diverse and abundant when compared to those of the short phenotype (Fig. 3a, Fig. 3b). In the root compartment, alpha-diversity and prokaryotic abundance were highest in the short phenotype (Fig. 3a, Fig. 3b). The root compartment showed a significant decline in alpha diversity in all plant phenotypes driven by a decrease in both richness and evenness when compared to their bulk and rhizospheric counterparts (Fig. 3a, Fig. 3c). Mean richness ± 95% confidence interval ($CI_{95\%}$) across microbiome compartments was 922 ± 40, 981 ± 33, and 695 ± 40 observed ASVs for bulk sediment, rhizosphere and root prokaryotic communities, respectively. Decreased evenness in the root compartment was evidenced by the presence of highly dominant ASVs (Fig. 3c). Despite the decrease in prokaryotic diversity in the root, abundance remained high, in the range of 10^7 SSU rRNA gene copies $g^{-1}_{\text{fresh root}}$ in both tall and short *S. alterniflora* phenotypes (Fig. 3b).

S. alterniflora phenotype and microbiome compartment were the most significant deterministic forces controlling prokaryotic community assembly in GA salt marshes (Fig. 3de, Table 1). PERMANOVA analysis using the Bray-Curtis dissimilarity index showed that *S. alterniflora*

168 phenotype explained less species exchange in the root when compared to the other two
169 compartments (Table 1).

170 Phylogenetic community structure was assessed with the nearest taxon index (NTI) and beta
171 nearest taxon index (βNTI) for within and between prokaryotic communities, respectively (Stegen
172 et al., 2012, 2013). An NTI value greater than 2 indicates greater phylogenetic clustering within a
173 community than expected by chance. All bulk and rhizospheric prokaryotic communities had an
174 NTI greater than 2; while 91% of the root prokaryotic communities met this threshold. NTI values
175 decreased in closer proximity to roots (Fig. S5). Average ± $CI_{95\%}$ NTI values per microbiome
176 compartment were 7.0 ± 0.3, 5.6 ± 0.2, and 3.8 ± 0.3 for prokaryotic communities from bulk
177 sediment, rhizosphere and root compartments, respectively. In order to assess phylogenetic
178 turnover between similar environments in the investigated salt marshes, βNTI values between
179 samples from the same microbiome compartment, *S. alterniflora* phenotype, year and location
180 were calculated. An βNTI value lower than -2 indicates less phylogenetic turnover between
181 samples than expected by chance. Pairwise comparison between bulk sediment, rhizosphere, and
182 root prokaryotic communities revealed that 92.2%, 92.6% and 77.8% βNTI values were below -2,
183 respectively. Similar to NTI analysis, a trend of lower phylogenetic relatedness was observed
184 closer to the root (Fig. S5). Average ± $CI_{95\%}$ βNTI was -5.2 ± 0.3, -4.6 ± 0.3, and -3.1 ± 0.2 in bulk
185 sediment, rhizosphere and root pairwise comparisons, respectively. The microbiome compartment
186 effect on NTI and βNTI was consistent in all *S. alterniflora* phenotypes.

187

188 2.3 *S. alterniflora* Root-associated prokaryotic community composition

189 Overall, at the phylum level, prokaryotic communities were predominated by ASVs from the
190 *Proteobacteria* (46.7%), *Chloroflexi* (15.2%), *Bacteroidetes* (8.4), *Epsilonbacteraeota* (3.7%),
191 *Spirochaetes* (3.6%), and *Acidobacteria* (3.5%) phyla (Fig. S6). At higher *S. alterniflora* biomass,
192 an increase in the relative abundance of *Proteobacteria* ASVs and a decline in the relative
193 abundance of *Chloroflexi* and *Spirochaetes* ASVs was observed (Fig. S6). At increasing proximity
194 from the root, the relative abundance of *Proteobacteria*, *Spirochaetes* and *Epsilonbacteraeota*
195 increased while *Acidobacteria* and *Bacteroidetes* decreased (Fig. S6). Prokaryotic taxa with the
196 potential to catalyze redox reactions in the S, Fe, and N cycles were investigated in greater detail
197 due to their known significance in salt marsh ecosystem functioning. Putative function was

inferred based on homology at the genus level with described prokaryotic species (Table S1). Prokaryotes putatively capable of nitrification (a.k.a. nitrifiers) exhibited higher relative abundance in areas colonized by the tall *S. alterniflora* phenotype, in comparison to areas occupied by the short and medium phenotypes (Fig. 4a). Dominant nitrifiers in the studied system included members of the bacterial genera *Candidatus* Nitrotoga and *Nitrospira*, as well as the archaeal genus *Candidatus* Nitrosopumilus (Fig. 4a). Additionally, a significant enrichment in taxa potentially involved in the Fe and S cycles were detected in the plant root relative to the bulk sediment (Fig. 4b,c,d). The putative Fe-oxidizer of the *Zetaproteobacteria*, *Mariprofundus* sp. showed high relative abundance in the roots of the tall *S. alterniflora* phenotype, while *Acidihalobacter* of the *Gammaproteobacteria* was the predominant Fe-oxidizer in the roots of the short phenotype (Fig. 4b). Putative autotrophic endosymbionts capable of S oxidation from the *Candidatus* Thiodiazotropha genus and *Thiomicrospirales* order preferably colonized the roots of *S. alterniflora* phenotypes regardless of plant phenotype (Fig. 4c). Sulfur oxidizers from the S*ulfurovum* genus preferentially colonized the areas dominated by the short *S. alterniflora* phenotype in all compartments (Fig. 4c). Putative sulfate-reducers of the *Desulfobacterales* order: *Desulfatitalea*, *Desulfopila*, and *Desulfosarcina* genera were enriched at closer proximities to the *S. alterniflora* root (Fig. 4d).

Based on differential abundance analysis performed in DESeq2, many ASVs were shown to be significantly enriched in the root compartment. Interestingly, many of the enriched taxa appear to be capable of N fixation, including putative sulfur oxidizers *Candidatus* Thiodiazotropha, *Desulfovibrio*, and *Arcobacter*, S/sulfate reducers *Sulfurospirillum,* and *Desulfatitalea*, and *Novosphingobium*, *Azoarcus*, and *Celerinatantimonas* bacteria (Fig. S7a). Taxa significantly enriched in the tall *S. alterniflora* phenotype comprised nitrifiers from the *Nitrospira* and *Candidatus* Nitrosopumilus genus, putative metal (Fe and Mn) reducer *Georgfuchsia*, and a diverse set of aerobic or facultative anaerobic chemoheterotrophs (Fig. S7b).

2.4 *S. alterniflora* core microbiome

Taxa consistently found in independent host microbiome samples have been suggested to perform key functions in healthy host-microbiome interactions (Shade and Handelsman, 2011), and the set of persistent taxa have been defined as the host's core microbiome. For this study, an ASV

prevalence threshold was operationally defined by plotting the relative abundance and richness of the rhizosphere and root core microbiomes at 10% intervals from 0% to 100% ASV prevalence cutoffs (Fig. S8). A conservative prevalence cutoff of 60% was determined by visually inspecting a threshold in which richness remained stable at increasing cutoff values (Fig. S8). The *S. alterniflora* core root microbiome was composed of only 38 out of 14,505 ASVs, and 54 out of 19,435 ASVs in the root and rhizosphere, respectively. However, in both cases the core microbiome comprised approximately 20% relative abundance of the total prokaryotic community (Fig. S8). Both the root and the rhizosphere core microbiomes were dominated by taxa with inferred metabolic potential for S redox reactions (Fig. 5). The *S. alterniflora* root core microbiome was comprised of putative autotrophic S oxidizers of the *Sulfurovum* and *Candidatus* Thiodiazotropha genera (Fig. 5), while sulfate reducers were represented by ASVs from the *Desulfatiglans*, *Desulfocarbo*, *Desulfatitalea*, *Desulfobulbus*, *Desulfopila*, *Desulfosarcina*, SEEP-SRB1 and Sva0081 genera (Fig. 5). Core root taxa with diazotrophic potential included ASVs from the *Candidatus* Thiodiazotropha, *Desulfatitalea*, *Desulfobulbus* and *Spirochaeta* genera (Fig. 5). In the rhizosphere, the proportion of ASVs with unknown classification at the genus level according to the SILVA database (release 132), comprised up to ~60% relative abundance of the core microbiome. Core rhizosphere ASVs with the putative capacity for S oxidation included members of the *Sulfurovum* and *Thioalkalispira* genera (Fig. 5). Similar to the root core microbiome, nearly half of the identified taxa at the genus level in the core rhizosphere presented sulfate reduction capability, such as ASVs from the *Desulfatiglans*, *Desulfocarbo*, *Desulfatitalea*, *Desulfosarcina*, SEEP-SRB1, and Sva0081 genera (Fig. 5). Putative nitrifiers from the *Candidatus* Nitrosopumilus genus were members of the rhizosphere core microbiome (Fig. 5). Finally, taxa with N fixation capability in the rhizosphere core microbiome included putative sulfur oxidizers from the *Thioalkalispira* genus, sulfate reducers from the *Desulfatitalea* genus, and bacterium from the *Spirochaeta* genus (Fig. 5).

3. Discussion

3.1. Biogeochemical processes linked to *S. alterniflora* primary productivity at the local scale

S. alterniflora primary productivity is strongly linked to N uptake kinetics in field and lab studies (Mendelssohn et al., 1979; Howes et al., 1986, Mendelssohn and Morris, 2000). At the local scale,

reduced, anoxic, and sulfidic root conditions were shown to lead to a decline in root energy status, affecting ammonium uptake kinetics (Koch et al., 1990; Mendelssohn and Morris, 2000). In parallel, elevated salinity has been associated with a decrease in stomatal conductance and photosynthetic activity, along with an increase in dark respiration (Giurgevich and Dunn, 1979; Hwang and Morris, 1994). Our observations corroborate these past results showing that *S. alterniflora* primary productivity is hampered at reduced sediment Eh and under highly sulfidic conditions, when the plants experience limited leaf gas exchange. Results from this study also support our previous research which revealed the dynamic interplay between the growth/physiology of macrophyte plants and macrofaunal bioturbation (Kostka et al., 2002a; Gribsholt et al., 2003), with crab burrow density shown to directly correlate with aboveground plant biomass and sediment redox potential (Fig S2).

Significant differences in stable N isotope composition of sediment and *S. alterniflora* leaves provide evidence that N sources and dynamics are distinct along the studied *S. alterniflora* primary productivity gradient (Craine et al., 2015). We argue that elevated leaf and sediment $\delta^{15}N$ in the tall *S. alterniflora* phenotype is the result of (i) greater nitrogen loss by coupled nitrification-denitrification, and (ii) differences in the source of N input. Denitrification in Georgia salt marshes is limited and tightly coupled to prokaryotic nitrification, which discriminates against ^{15}N (Dollhopf et al., 2005, Craine et al., 2015). Prokaryotes capable of nitrification show higher relative abundance in sediments dominated by the tall *S. alterniflora* phenotype (Fig. 4a), and their activity is known to be inhibited by sulfide toxicity (Joye and Hollibaugh, 1995; Dollhopf et al., 2005). Porewater sulfide concentration in the short and medium *S. alterniflora* phenotype was an order of magnitude higher than in the tall phenotype. A second explanation for $\delta^{15}N$ enrichment in the tall *S. alterniflora* phenotype is the greater source of planktonic N at closer proximities to the tidal creek. Planktonic tissue has a $\delta^{15}N$ signature of 8.6 ± 1.0 ‰ (Peterson, 1999), which is more similar to the leaf $\delta^{15}N$ measured in the tall *S. alterniflora* (7.6 ± 0.3 ‰) when compared to the short phenotype (5.5 ± 0.4 ‰) (Fig. S4). A larger discrepancy in $\delta^{13}C$ between sediment and leaf tissue in the tall *S. alterniflora* phenotype, as well as a lower sediment C:N ratio, support our interpretation of a reduced relative contribution of vascular plant material to organic matter diagenesis (Fig. S4; Ember et al., 1987; Fig. 1b, Gebrehiwet et al., 2008). The average ± $CI_{95\%}$ $\delta^{13}C$ signature in sediments from the tall *S. alterniflora* phenotype (-20.3 ± 0.4 ‰) more closely resembles that of reported phytoplankton, which enters the marsh via tidal creeks (-17 to -24‰,

Fogel et al., 1989; -21.3 ± 1.1 ‰, Peterson, 1999; -20.16 ‰, Dai et al., 2005). The C:N ratio is considered as a proxy for soil organic matter reactivity, and a lower C:N ratio indicates a greater potential for rapid biodegradation and N mineralization (Janssen, 1996). In agreement with this interpretation, sediments with low C:N ratios from the tall *S. alterniflora* zone contained higher prokaryotic biomass, and higher rates of extracellular enzyme activities involved in the C, N, and P cycles. We propose that plant primary productivity is enhanced in the tall *S. alterniflora* zone in part due to more rapid microbial mineralization of higher-quality sediment organic matter of planktonic origin, with released inorganic nutrients then made available for plant uptake.

3.2. Assembly of the *S. alterniflora* root microbiome:

Previous studies have reported contradictory results with regard to the relationship between the diversity of the *S. alterniflora* microbiome, plant productivity, and proximity to the root (Zogg et al., 2018; Lin et al., 2019; Kolton et al., 2020). Our finding of higher prokaryotic alpha diversity in bulk and rhizospheric sediment associated with the tall *S. alterniflora* phenotype is consistent with previous findings from Skidaway Island, GA (Kolton et al. 2020). However, Zogg et al. (2018) and Lin et al., (2019) did not observe significant differences in prokaryotic alpha diversity between the tall and short *S. alterniflora* phenotypes in bulk and rhizospheric sediments from New England and Guangdong province in China, respectively. Contrasting results could be due to limitations in methodology and experimental design in previous work. Sequencing platforms continue to evolve, enabling higher sequence coverage at lower cost, and our sampling effort was approximately an order of magnitude more intensive than previous studies characterizing the *S. alterniflora* root microbiome, including our own past work (Zogg et al., 2018; Lin et al., 2019; Kolton et al., 2020). Moreover, recently developed *in silico* technology to infer ASVs instead of clustering sequences into operational taxonomic units (OTUs) could also impact the estimation of alpha diversity metrics.

Few studies have investigated microbial diversity in the roots of wetland plant roots. Nonetheless, consistent with our results, a single report from *S. alterniflora* and studies from other wetland/estuarine plants show a decline in diversity in the root compared to the bulk and rhizosphere compartments (Edwards et al., 2015; Hong et al., 2015; Martin et al., 2020a). Prokaryotic abundance in the endosphere has been previously estimated in the 10^4 to 10^8 cells g^{-1}

range across an array of plant species (Bulgarelli et al., 2013). Taking into consideration that many of these previous estimates employed cultivation-based methods, and prokaryotic genomes often contain multiple SSU rRNA operons, our observation of prokaryotic abundance (10^7 SSU rRNA gene copies g^{-1}) would be placed at the high-end of that range. A marked decrease in prokaryotic alpha diversity with high abundances is an indication that the *S. alterniflora* root compartment is enriched in dominant and highly active species taking advantage of labile carbon sources, reduced inorganic compounds, and the oxidized environment found in the *S. alterniflora* root (Carlson and Forrest, 1982; Maricle and Lee, 2002). Increased relative abundances of S and Fe chemolithotrophs, and aerobic and facultative anaerobic chemoorganotrophs at closer proximities to the root further support this interpretation.

Microbial community assembly in the root endosphere has been proposed as a two-step colonization process (Bulgarelli et al., 2013). The first step is driven by microbial proliferation in the rhizosphere by species capable of utilizing plant-released substrates; while the second is a fine-tuning step in the rhizoplane, where selection by the plant´s genotype-dependent immune system takes place (Bulgarelli et al., 2013). Endospheric microbial species have co-evolved to evade the plant immune system by secreting effector proteins that mimic plant proteins (Trivedi et al., 2020). In *S. alterniflora*, a decrease in prokaryotic richness in the root compartment, and the fact that plant phenotype was the most important deterministic factor assembling the root prokaryotic community, suggest that plant selection is an important process in community assembly. However, community assembly is a result of co-occurring deterministic and stochastic processes (Stegen et al., 2013; Dini-Andreote et al., 2015). Generally, environmental filtering has been shown to be the main deterministic process assembling microbial communities spatially, as evidenced by phylogenetic clustering (Stegen et al., 2012; Freedman and Zak, 2015). Nevertheless, in our study, environmental filtering was relaxed at closer proximity to the root, a microenvironment characterized by an abundance of high-quality e^- donors and acceptors. Most likely, increased competition, the dominance of fast-growing bacteria filling a resource-rich niche, and historical contingency (i.e., first prokaryotic species to colonize the root successfully outcompete other taxa) are co-occurring ecological processes reducing the relative importance of environmental filtering in the root zone (Fukami, 2015; Hassani et al., 2018; Toju et al., 2018). Increased species dominance, decreased richness, and increased phylogenetic dispersion with high prokaryotic abundances in the *S. alterniflora* root supports this hypothesis.

3.3. Characterization of the *S. alterniflora* core microbiome and potential plant-microbe interactions driving primary productivity

Our results indicate that putative sulfate-reducing and sulfur-oxidizing prokaryotes comprise a large proportion of the *S. alterniflora* root and rhizosphere core microbiomes. Sulfate-reducing communities are comprised of metabolically versatile populations capable of utilizing a broad range of C substrates, including plant-derived substrates (Bahr et al., 2005). The most dominant sulfate-reducer genus in the *S. alterniflora* core root and rhizosphere, *Desulfatitalea*, mainly utilizes short-chain fatty acids as an electron donor and C source (Higashioka et al., 2013). However, other sulfate-reducing members of the root core microbiome such as *Desulfatiglans* and *Desulfocarbo*, have been shown to oxidize plant-derived aromatic compounds (e.g., lignin) (An and Picardal, 2014; Suzuki et al., 2014). In salt marsh ecosystems, biogeochemical data indicates that the C and S cycles are tightly coupled, with *S. alterniflora* photosynthetic activity fueling the activity and C utilization of sulfate-reducers in the rhizosphere (Kostka et al., 2002b; Hyun et al., 2007; Spivak and Reeve, 2015). Similarly, sulfide-oxidizers thrive in the *S. alterniflora* root zone, especially in the short phenotype, where sulfide concentration is elevated (Thomas et al., 2014; Kolton et al., 2020; this study). In our study, ASVs from the *Sulfurovum* genus were enriched in all compartments of the short *S. alterniflora* phenotype. This genus has been described as highly versatile and diverse, allowing for efficient niche partitioning in highly dynamic sulfidic and oxic environments (Meier et al., 2017; Moulana et al., 2020). The co-occurrence of prokaryotic ASVs associated with S anaerobic and aerobic metabolisms in the *S. alterniflora* rhizosphere and root, and highly dynamic O_2 concentrations at the microscale (Koop-Jakobsen et al., 2018), support the interpretation of a rapid and cryptic S cycle at close proximity to, or even inside, the root tissue. Rapid and coupled cycling of C and S are crucial to the replenishment of nutrients and electron acceptors in the *S. alterniflora* root-zone to support high microbial and plant activity. Rapid organic matter mineralization is especially relevant to effectively recycle N, most often the limiting nutrient for plant productivity in the salt marsh (subsection 3.1).

Previous studies in marshes of the southeastern US show that plant photosynthetic activity and rhizodeposition stimulate N fixation by root-associated sulfate reducers (Whiting et al., 1986; Gandy and Yoch, 1988; Lovell et al., 2000). Consistently, prokaryotic species from the

Desulfobulbus, Desulfatitalea, *Desulfovibrio,* and *Sulfurospirillum* genera, either significantly enriched or members of the *S. alterniflora* root core microbiome, have been shown to couple sulfate or sulfur respiration to N fixation (Higashioka et al., 2015; Thajudeen et al., 2017). Species from the root and rhizosphere core microbiome genera *Candidatus* Thiodiazotropha and *Thioalkalispira* have the metabolic potential to couple S oxidation with C and N fixation (Barbieri et al., 2010; Petersen et al., 2016). Intriguingly, *Candidatus* Thiodiazotropha is a recently described genus of endosymbionts discovered in the gills of lucinid bivalves (Petersen et al., 2016). Lucinid bivalves are not generally found in salt marshes, but they have been associated with reduced plant sulfide stress in seagrass meadows and mangroves (Lim et al., 2019a; Lim et al., 2019b; Gagnon et al., 2020). In these ecosystems, a tripartite symbiotic relationship occurs, whereby bivalves provide O_2 to endosymbiont sulfide-oxidizers that detoxify the plant's environment from sulfide, a known phytotoxin (Gagnon et al., 2020). Recent studies revealed that *Candidatus* Thiodiazotropha is also an important and prevalent member of the seagrass root microbiome, suggesting that these chemolithoautotrophic S oxidizers form a direct association with subtidal marine plant species without the need of a lucinid bivalve partner (Crump et al., 2018; Martin et al., 2020b). Our study confirms this finding, and expands the distribution range of *Candidatus* Thiodiazotropha to the roots of intertidal, estuarine plant species.

Although sulfide is generally considered as a potent phytotoxin, slightly sulfidic conditions (< 1 mM) have been shown to actually stimulate *S. alterniflora* growth in a controlled laboratory experiment (Morris et al., 1996). Energy conservation from sulfide oxidation in the root tissue was speculated to be the driver of increased plant primary production (Mendelssohn and Morris, 2000). Further, sulfide oxidation to sulfate has been demonstrated inside *S. alterniflora* root tissues using isotope tracers (Carlson and Forrest, 1982; Lee et al., 1999). However, it is still not clear what process, biological or chemical, dominates sulfide oxidation inside *S. alterniflora* roots. We propose that *S. alterniflora* shares a symbiotic relationship with S oxidizers in both the rhizosphere and root compartments. Sulfur oxidation may be mediated not only by *Candidatus* Thiodiazotropha bacteria, but also members of the *Sulfurovum* and *Thioalkalispira* genera, or endosymbionts from the *Thiomicrospirales* order. Previously studied microbial species from the *Sulfurovum* genus and endosymbionts from the *Thiomicrospirales* order have been demonstrated to fix C; whereas members from *Desulfovibrio*, *Thioalkalispira*, and *Candidatus* Thiodiazotropha genera have been shown to perform both C and N fixation (Barbieri et al., 2010; Petersen et al.,

2016; Suzuki et al., 2006; Thajudeen et al., 2017). Moreover, Crump et al. (2018) studying the root microbiome of seagrass *Zostera* spp., found high transcripts levels of N fixing and sulfur oxidizing genes from *Gammaproteobacteria* species, including endosymbionts of marine invertebrate from the *Sedimenticolaceae* family, which includes the *Candidatus* Thiodiazotropha genus. Given that the *S. alterniflora* root zone is enriched in reduced S and its growth is limited by N uptake, we suggest that diazotrophy coupled to sulfide oxidation may be a key process that was previously overlooked. However, direct measurements of N and C fixation, and sulfur oxidation in the roots of *S. alterniflora*, their rates and controls, along with their relative contribution to plant growth remain unclear and require further research. Given that most studies, including this study, have inferred the coupling of S oxidation and N fixation based on gene homology and/or taxonomic placement, this interpretation should be treated with caution.

4. Conclusions

We studied a gradient in *S. alterniflora* productivity to characterize the ecology and physiology of the *S. alterniflora* root-associated microbiome, and its potential role shaping plant physiological performance. In sediments from the tall *S. alterniflora* phenotype, higher prokaryotic biomass and more rapid microbial mineralization of organic matter was linked to greater inorganic nutrients replenishment for plant uptake. Prokaryotic communities from bulk and rhizospheric sediment associated with the tall *S. alterniflora* phenotype contained the highest alpha diversity; while a decline in diversity was observed in the root in comparison to the to bulk and rhizosphere sediment compartments in all *S. alterniflora* phenotypes. A marked decrease in prokaryotic alpha diversity with high abundances and increased phylogenetic dispersion was observed in the *S. alterniflora* root compartment. Thus, we propose that the *S. alterniflora* root microbiome is dominated by highly active and competitive species taking advantage of available carbon substrates in the oxidized root zone. The high relative abundance of prokaryotic ASVs with putative S oxidation and sulfate reduction capability in the *S. alterniflora* rhizosphere and root suggests a rapid S cycle at close proximity to, or even inside, the root tissue. Moreover, both functional guilds were overrepresented in the *S. alterniflora* rhizosphere and root core microbiome. Rapid recycling of S is crucial for organic matter mineralization in anoxic marsh sediments. Thus, we propose that *S. alterniflora* shares a symbiotic relationship with S oxidizing bacteria in both the rhizosphere and root compartments. Sulfur oxidizers may benefit *S. alterniflora* plants not only by removing potentially toxic sulfide from the root zone, but also by coupling S oxidation with N and/or C

fixation. The contribution to plant growth of each of these microbial processes represents a knowledge gap that warrants further research.

5. Materials and methods

5.1 Sampling design and general site description

The study was carried out in two salt marshes for which long-term data is available in the state of Georgia, USA: (i) the Georgia Coastal Ecosystem - Long Term Ecological Research (GCE-LTER) site 6 at Sapelo Island (Lat: 31.389° N, Long: 81.277° W), and (ii) the Saltmarsh Ecosystem Research Facility (SERF) adjacent to the Skidaway Institute of Oceanography on Skidaway Island (Lat: 31.975° N, Long: 81.030° W) (Fig. S1). The GCE-LTER site was sampled twice, during July 2018 and 2019, while the SERF site was sampled once in July 2019. Four ~100 m transects adjacent to large tidal creeks with two to four sampling points along *S. alterniflora* primary productivity gradients were sampled at each site (total: 24 sampling points, Fig. S1).

At each sampling point along the transects, a 50 cm x 50 cm quadrat was established to measure the density of marsh periwinkle snails (*Littoraria irrorata*), and fiddler crab (*Uca pugnax*) burrows. *In-situ* sediment pH and redox potential (Eh) were measured in triplicate at two sediment depths (2.5 and 7.5 cm) with a hand-held pH/ORP meter during the two sampling events at Sapelo Island (HI-98121 tester, Hanna instruments, Woonsocket, RI, USA).

5.2 *S. alterniflora* ecophysiology and elemental analysis

S. alterniflora shoot density was quantified at every sampling point in 50 cm x 50 cm quadrats, and shoot height measured for 10 plants per sampling point. *S. alterniflora* plants were operationally classified in three phenotypes based on shoot height: short (< 50 cm), medium (50 – 80 cm) and tall (> 80 cm). *S. alterniflora* shoot biomass was estimated by allometry, with an equation calibrated at Sapelo Island (Table S2, Wieski and Pennings, 2014). During the 2019 sampling events, leaf C and N concentration and ^{13}C and ^{15}N isotopic natural abundance were determined for 3 plants per sampling point with elemental and isotope analyses conducted at the University of Georgia – Center for Applied Isotope Studies (CAIS https://cais.uga.edu/). Leaf elemental analysis was performed by the micro-Dumas method, while isotopic natural abundance was measured by isotope ratio mass spectrometry. ^{13}C natural abundance was expressed as the per

mille (‰) deviation from the Pee Dee Belemnite standard (PDB) ^{13}C:^{12}C ratio ($\delta^{13}C$); while ^{15}N natural abundance expressed as the ‰ deviation from the N_2 atmospheric ^{15}N:^{14}N ratio ($\delta^{15}N$). Leaf temperature, a proxy for stomatal conductance (Ramírez et al., 2016), was measured between 11:00 and 12:00 utilizing a Fluke-62 MAX+ infrared thermometer (Fluke Co. USA, Everett, WA). All leaf ecophysiological measurements were performed in young, expanded, and sun exposed leaves.

5.3 Porewater and sediment sampling and chemical analysis

Rhizon samplers with 0.15 µm pore size filters (model CSS, Rhizosphere Research Products, Wageningen, The Netherlands, https://www.rhizosphere.com/rhizons), were used to extract sediment porewater at 2.5 and 7.5 cm depth from every sampling point. For each porewater sample, a 2 ml subsample was frozen at -20ºC for salinity, nitrate, ammonium, and phosphate concentration analysis; a 2 ml subsample was immediately acidified with 20 µL 12N HCl for Fe^{2+} and Fe^{3+} concentration analysis; and a 100 µL subsample was immediately fixed into 1 ml zinc acetate 2% (w/v) solution for sulfide concentration analysis (Kostka et al., 2002a; Hyun et al., 2007).

Porewater concentrations of nitrate, ammonium, phosphate, sulfide, Fe^{3+}, and Fe^{2+} were quantified based on spectrophotometric methods as previously described (Watanabe and Olsen 1965, Cline 1969, Stookey 1970; Sims et al. 1995; Garcia-Robledo et al. 2014). Porewater chloride concentration was determined by HPLC with ultraviolet detection as described by Beckler et al. (2014). Salinity was calculated based on porewater chloride concentration.

Sediment samples were collected at all sampling points from two depth intervals, 0-5 cm and 5-10 cm. An approximately 30 g sediment subsample was oven-dried at 60ºC for 72 hours. The oven-dried sample was homogenized using a PowerGen high throughput homogenizer (Fisherbrand, Pittsburgh, PA) and sent to the University of Georgia CAIS (https://cais.uga.edu/) for organic C and N concentration and ^{13}C and ^{15}N isotopic natural abundance analyses. Sediment organic C and ^{13}C isotopic natural abundance was analyzed in acid-fumigated samples (Ramnarine et al., 2011).

Samples collected for microbial community analysis were flash-frozen in an ethanol and dry ice bath, and stored at -80ºC until nucleic acid extraction. Sediment samples collected for enzymatic rates were kept at 4 ºC, and analyzed within 4 hours after sampling.

500

501 5.4 Extracellular enzyme activity

502 Rates of extracellular enzymatic activity (β-glucosidase, phosphatase, and chitinase) were
503 measured in 2019 in Sapelo and Skidaway Island. Technical duplicates of 0-10 cm deep sediment
504 samples were collected for each sampling point. Rates were analyzed in a homogenized sediment
505 slurry using fluorescent 4-methylumbelliferone (MUF) linked-substrates (Table S3). Slurry
506 preparation consisted of mixing wet sediment with 50 mM Tris buffer (pH 7) in a 1:2 (w/v) ratio.
507 The slurry was homogenized with a stomacher homogenizer (model 400; Seward Medical,
508 London, England) at 200 rpm for 30 s in ~1-mm filter bags. Sediment slurry (800 µL) was
509 incubated in the dark with 200 µL of fluorescent-linked substrate (initial substrate concentration:
510 40 µM). Product accumulation was measured at 0, 0.5, 1, 1.5, 3, 4, 6 and 8 hours after start of the
511 incubation based on fluorescence intensity (excitation: 355 nm, emission: 460 nm) using a
512 microplate fluorescence reader (SpectraMax M2, Molecular Devices, San Jose, CA). Enzymatic
513 rates were calculated by fitting a linear regression, and reported in µmol $kg_{wet\ sediment}^{-1}$ h^{-1}.

514

515 5.5 Plant sampling, compartment fractionation, and molecular biology

516 *S. alterniflora* roots were sampled at two depths (0-5 and 5-10 cm). Sediment loosely attached to
517 the root was immediately washed two times with creek water in the field. Roots with remaining
518 rhizospheric sediment were flash frozen in an ethanol-dry ice bath and stored at -80ºC until
519 analysis.

520 5.5.1 Plant compartment separation

521 Separation of the root and rhizosphere compartments was performed by sonication in an epiphyte
522 removal buffer (0.1% (v/v) Triton X-100 in 50 mM potassium-phosphate buffer) (Simmons et al.
523 2018). Sonication was performed at 4ºC for 10 minutes with pulses of 160W for 30 s interspersed
524 with 30 s pauses. Sediment detached from the roots was centrifuged and considered to be the
525 rhizosphere compartment, while the sonicated roots were considered as the root compartment. The
526 root compartment was washed with PBS buffer (pH 7.4) three consecutive times, and ground with
527 liquid N before DNA extraction. Simmons et al. (2018) protocol was designed to isolate

endospheric DNA; however, since we did confirm the separation by microscopy, it is possible that our root compartment contained residues of the rhizoplane compartment.

5.5.2 Removal of extracellular DNA

Prior to bulk sediment DNA extraction, extracellular dissolved or sediment-adsorbed DNA was removed according to Lever et al. (2015). Briefly, 2 g of sediment was incubated with 2 ml carbonate dissolution solution (0.43 M sodium acetate, 0.43 M acetic acid, 10 mM EDTA, 100 mM sodium metaphosphate, 3% (w/v) NaCl, pH 4.7) for 1 hour while orbital shaking at 300 rpm and room temperature. Afterwards, 16 ml of a 300mM Tris-HCl and 10mM EDTA solution (3% NaCl, pH 10.0) was added into the slurry and incubated for 1 additional hour at the same orbital shaking condition. After centrifugation at 10,000 g for 20 minutes at room temperature, the pellet was composed by extracellular-DNA free sediment and used for prokaryotic community characterization.

5.5.3 DNA extraction and sequencing library preparation

DNA extraction for all assessed compartments was performed using the DNeasy PowerSoil kit (Qiagen, Valencia, CA) according to the manufacturer's protocol. The concentration of extracted DNA was determined with the Qubit HS assay (Invitrogen, Carlsbad, CA). Amplification of the SSU rRNA gene V4 region was performed using the primers 515F (5'-GTGCCAGCMGCCGCGGTAA') and 806R (5'-GGACTACHVGGGTWTCTAAT') (Caporaso et al., 2011). Reactions were performed in triplicate of 5 ng DNA template in a solution containing DreamTaq buffer, 0.2 mM dNTPs, 0.5 µM of each primer, 0.75 µM of each mitochondrial (mPNA) and plastid (pPNA) peptide nucleic acid (PNA) clamps, and 1.25 U DreamTaq DNA polymerase as previously described (Kolton et al 2020, further details in Table S4). PNA clamps have been shown to reduce plant plastid and mitochondrial DNA amplification in PCR reactions (Lundberg et al., 2013). Triplicate PCR products were pooled together, barcoded with 10-base unique barcodes (Fluidigm Corporation, San Francisco, CA), and sequenced on an Illumina MiSeq2000 platform using a 500-cycle v2 sequencing kit (250 paired-end reads) at the Research Resources Center in the University of Illinois at Chicago. The raw SSU rRNA gene amplicon sequences have been deposited in the BioProject database (http://ncbi.nlm.nih.gov/bioproject) under accessions PRJNA666636.

558 5.6 Quantification of prokaryotic abundance

559 Prokaryotic abundance was quantified by quantitative polymerase chain reaction (qPCR) of the
560 SSU rRNA gene with general primers in a subset of 24 samples collected in Sapelo Island in 2018
561 and 2019. The subset comprised superficial (0-5 cm) samples from all three compartments,
562 collected from the four established transects in Sapelo Island. Only sample from the tall and short
563 extreme *S. alterniflora* phenotypes were included into the analysis. Samples were analyzed in
564 triplicate using the StepOnePlus platform (Applied Biosystems, Foster City, CA, United States)
565 and PowerUp SYBR Green Master Mix (Applied Biosystems, Foster City, CA, United States).
566 Reactions were performed in a final volume of 20µl using the standard primer set 515F (5'-
567 GTGCCAGCMGCCGCGGTAA') and 806R (5'-GGACTACHVGGGTWTCTAAT') specific for
568 the prokaryotic SSU rRNA gene (Caporaso et al., 2011, Table S4). To avoid plant plastid and
569 mitochondrial DNA amplification from rhizosphere and root samples, peptide nucleic acid PCR
570 blockers (PNA clamps, 0.75 µM) were added to all qPCR reactions (Lundberg et al., 2013).
571 Standard calibration was performed from a 10-fold serial dilution (10^3 to 10^8 molecules) of
572 standard pGEM-T Easy plasmids (Promega, Madison, WI, United States) containing target
573 sequences from *Escherichia coli* K12. Specificity of PCR products was confirmed by melting
574 curve analyses. Prokaryotic SSU rRNA gene copy numbers were calculated as gene copy number
575 g^{-1} of fresh material.

576

577 5.7 Ecological, phylogenetic, statistical and bioinformatic analysis

578 Amplification primers were removed from raw fastq files using Cutadapt v.2.0 (Martin, 2011).
579 Amplicon sequence variants (ASVs) were inferred from quality filtered reads utilizing DADA2
580 v.1.10 (Callahan et al., 2016). Paired reads were merged, and reads between 251 and 255 bp length
581 were conserved. Chimeras were removed using the removeBimeraDenovo function from the
582 DADA2 package. Taxonomy was assigned utilizing the RDP Naive Bayesian Classifier (Wang et
583 al., 2007) against the SILVA SSU rRNA reference alignment (Release 132, Quast et al., 2013).
584 Sequences classified as chloroplast, mitochondrial, eukaryotic, or that did not match any
585 taxonomic phylum were excluded from the dataset. Reads were filtered to remove ASVs that
586 appeared in less than 5% of the samples and/or had less than 10 total counts. A total of 32,740
587 unique ASVs were aligned to the SILVA SSU rRNA reference alignment (Release 132, Quast et

al., 2013) in mothur v.1.43 (Schloss et al., 2009), and an approximately maximum-likelihood tree was constructed using FastTree v.2.1 (Price et al., 2010). Finally, 10,068,980 high quality SSU rRNA sequence reads with a median depth of 49,619 reads per sample were used for subsequent analysis.

Shannon diversity index was estimated using the phyloseq v.1.26 package (McMurdie and Holmes, 2013). Non-metric multidimensional scaling (nMDS) ordination utilizing the Bray-Curtis dissimilarity distance was performed. Multivariate variation of the Bray-Curtis dissimilarity matrix was partitioned to microbiome compartment (bulk sediment, rhizosphere, and root), *S. alterniflora* phenotype (tall, medium, and short), depth (0-5 cm, and 5-10 cm), location (Sapelo Island, and Skidaway Island), and year (2018, and 2019) based on a PERMANOVA analysis with 999 permutations performed in vegan v. 2.5 (Oksanen et al. 2013). PERMANOVA analysis was run for the complete dataset and in subsets per microbiome compartment. Differential abundance analysis was performed to assess genera that were significantly enriched in specific plant compartments, and in zones of the marsh associated with different *S. alterniflora* phenotypes, using DESeq2 v.1.26 (Love et al., 2014).

To evaluate phylogenetic community structure within (alpha) and between (beta) communities, we quantified the nearest taxon index (NTI) and the beta nearest taxon index (βNTI), respectively (Stegen et al., 2012, 2013). NTI and βNTI indices were calculated as the number of standard deviations of the observed mean-nearest-taxon-distance (MNTD) and βMNTD from a null distribution (999 randomizations of all ASVs names across phylogenetic tree tips) using the picante package v. 1.8 (Kembel et al., 2010). For within community analysis, an NTI greater than +2 indicates that coexisting taxa are more closely related than expected by chance (phylogenetic clustering due to environmental filtering); while an NTI less than -2 indicates that coexisting taxa are more distantly related than expected by chance (phylogenetic overdispersion due to greater competition between closely related ASVs) (Stegen et al., 2012). For βNTI, we assessed pairwise comparisons for samples from the same plant compartment, *S. alterniflora* phenotype, and sampling event in order to evaluate if phylogenetic structure within communities (NTI) replicated at a greater scale (βNTI between samples occupying the same marsh microenvironment). A βNTI value <-2 or >+2 indicates less or greater than expected phylogenetic turnover between two samples than expected by chance, respectively (Stegen et. al., 2012).

The *S. alterniflora* core root microbiome was investigated. For this study, an ASV prevalence threshold was operationally defined by plotting the relative abundance and richness of the rhizosphere and root core microbiomes at 10% intervals from 0% to 100% ASV prevalence cutoffs (Fig. S8). A conservative prevalence cutoff of 60% was determined by visually inspecting a threshold in which richness remained stable at increasing cutoff values (Fig. S8). Finally, putative nitrifying, S oxidizing, S/sulfate reducing, and Fe oxidizing function was inferred based on homology of ASVs at the genus level with previously described prokaryotic species (Table S1).

DATA AVAILABILITY

Sequence data is available in the BioProject database (http://ncbi.nlm.nih.gov/bioproject) under accessions PRJNA666636. Associated data and metadata, and R script for bioinformatic pipeline used in this study is available in https://github.com/kostka-lab/Spartina_GA_Core_Microbiome

COMPETING INTERESTS

The authors declare that they have no competing interests

AUTHORS CONTRIBUTIONS

J.L.R., M.K. and J.E.K conceived of the study; J.L.R., M.K., T.S., J.E.K collected samples from the field; J.L.R., and M.K. performed the experiment, and the data analyses. J.L.R., M.K. and J.E.K., wrote the manuscript; J.L.R., M.K. T.S., and J.E.K., provided valuable insight and ideas during numerous sessions of discussion. All authors provided critical comments on the manuscript and gave final approval for publication.

FUNDING

This work was supported in part by an institutional grant (NA18OAR4170084) to the Georgia Sea Grant College Program from the National Sea Grant Office, National Oceanic and Atmospheric Administration, U.S. Department of Commerce and by a grant from the National Science Foundation (DEB 1754756). Any opinions, findings and conclusions or recommendations expressed in this material are those of the authors and do not necessarily reflect the views of the National Science Foundation.

ACKNOWLEDGMENTS

Authors would like to acknowledge Christina Stoner and Jack Cenatempo, as well as teachers from the GCE Schoolyard Program for their field work assistance. This is contribution 1087 of the University of Georgia Marine Institute.

REFERENCES

1. An, T.T., Picardal, F.W., 2014. *Desulfocarbo indianensis* gen. nov., sp. nov., a benzoate-oxidizing, sulfate-reducing bacterium isolated from water extracted from a coal bed. International journal of systematic and evolutionary microbiology, 64:2907-2914.
2. Bahr, M., Crump, B.C., Klepac-Ceraj, V., Teske, A., Sogin, M.L., Hobbie, J.E., 2005. Molecular characterization of sulfate-reducing bacteria in a New England salt marsh. Environmental Microbiology, 7:1175-1185.
3. Barbier, E.B., Hacker, S.D., Kennedy, C., Koch, E.W., Stier, A.C., Silliman, B.R., 2011. The value of estuarine and coastal ecosystem services. Ecological Monographs, 81:169-193.
4. Barbieri, E., Ceccaroli, P., Saltarelli, R., Guidi, C., Potenza, L., Basaglia, M., et al., 2010. New evidence for nitrogen fixation within the Italian white truffle Tuber magnatum. Fungal biology, 114:936-942.
5. Beckler, J.S., Nuzzio, D.B., Taillefert, M., 2014. Development of single-step liquid chromatography methods with ultraviolet detection for the measurement of inorganic anions in marine waters. Limnology and Oceanography: Methods 12:563-576.
6. Bradley, P.M., Morris, J.T., 1990. Influence of oxygen and sulfide concentration on nitrogen uptake kinetics in *Spartina alterniflora*. Ecology, 71:282-287.
7. Brown, M. M., Friez, M. J., Lovell, C. R., 2003. Expression of nifH genes by diazotrophic bacteria in the rhizosphere of short form *Spartina alterniflora*. FEMS Microbiology Ecology, 43:411-417.
8. Bulgarelli, D., Schlaeppi, K., Spaepen, S., Van Themaat, E.V.L., Schulze-Lefert, P., 2013. Structure and functions of the bacterial microbiota of plants. Annual review of plant biology, 64:807-838.
9. Callahan, B.J., McMurdie, P.J., Rosen, M.J., Han, A.W., Johnson, A.J., Holmes, S.P., 2016. DADA2: High-resolution sample inference from Illumina amplicon data. Nature methods 13:581–583.
10. Caporaso, G., Lauber, C.L., Walters, W.A., Berg-Lyons, D., Lozupone, C.A., Turnbaugh, P.J., Fierer, N., Knight, R., 2011. Global patterns of 16S rRNA diversity at a depth of millions of sequences per sample. PNAS 108:4516-4522.
11. Carlson, P.R., Forrest, J., 1982. Uptake of dissolved sulfide by *Spartina alterniflora*: Evidence from natural sulfur isotope abundance ratios. Science, 216:633-635.
12. Cline, J.D., 1969. Spectrophotometric determination of hydrogen sulfide in natural waters. Limnol. Oceanogr. 14:454–458.

683 13. Craine, J.M., Brookshire, E.N.J., Cramer, M.D., Hasselquist, N.J., Koba, K., Marin-
684 Spiotta, E., Wang, L., 2015. Ecological interpretations of nitrogen isotope ratios of
685 terrestrial plants and soils. Plant and Soil, 396:1-26.

686 14. Crump, B.C., Wojahn, J.M., Tomas, F., Mueller, R.S., 2018. Metatranscriptomics and
687 Amplicon Sequencing Reveal Mutualisms in Seagrass Microbiomes. Frontiers in
688 Microbiology, 9:388.

689 15. Dai, J., Sun, M.-Y., Culp, R.A., Noakes, J.E., 2005. Changes in chemical and isotopic
690 signatures of plant materials during degradation: Implication for assessing various organic
691 inputs in estuarine systems. Geophysical Research Letters, 32: L13608.

692 16. Davis, D. A., Gamble, M. D., Bagwell, C. E., Bergholz, P. W., Lovell, C. R., 2011.
693 Responses of salt marsh plant rhizosphere diazotroph assemblages to changes in marsh
694 elevation, edaphic conditions and plant host species. Microbial ecology, 61:386-398.

695 17. Dini-Andreote, F., Stegen, J.C., van Elsas, J.D., Salles, J.F., 2015. Disentangling
696 mechanisms that mediate the balance between stochastic and deterministic processes in
697 microbial succession. Proceedings of the National Academy of Sciences, 112:E1326-
698 E1332.

699 18. Dollhopf, S.L., Hyun, J.H., Smith, A.C., Adams, H.J., O'Brien, S., Kostka, J.E., 2005.
700 Quantification of ammonia-oxidizing bacteria and factors controlling nitrification in salt
701 marsh sediments. Applied and Environmental Microbiology, 71:240-246.

702 19. Dubilier, N., Bergin, C., Lott, C., 2008. Symbiotic diversity in marine animals: the art of
703 harnessing chemosynthesis. Nature Reviews Microbiology, 6:725-740.

704 20. Edwards, J., Johnson, C., Santos-Medellín, C., Lurie, E., Podishetty, N.K., Bhatnagar, S.,
705 Eisen, J.A., Sundaresan, V., 2015. Structure, variation, and assembly of the root-associated
706 microbiomes of rice. Proceedings of the National Academy of Sciences, 112:E911-E920.

707 21. Ember, L.M., Williams, D.F., Morris, J.T., 1987. Processes that influence carbon isotope
708 variations in salt marsh sediments. Marine Ecology Progress Series, 36:33-42.

709 22. Fogel, M. L., Sprague, E. K., Gize, A. P., Frey, R. W., 1989. Diagenesis of organic matter
710 in Georgia salt marshes. Estuarine, Coastal and Shelf Science, 28:211-230.

711 23. Freedman, Z., Zak, D.R., 2015. Soil bacterial communities are shaped by temporal and
712 environmental filtering: evidence from a long-term chronosequence. Environmental
713 microbiology, 17:3208-3218.

714 24. Fukami, T., 2015. Historical contingency in community assembly: integrating niches,
715 species pools, and priority effects. Annual Review of Ecology, Evolution, and Systematics,
716 46:1-23.

717 25. Gagnon, K., Rinde, E., Bengil, E.G., Carugati, L., Christianen, M.J., Danovaro, R., Gambi,
718 C., Govers, L.L., Kipson, S., Meysick, L., Pajusalu, L., 2020. Facilitating foundation
719 species: The potential for plant–bivalve interactions to improve habitat restoration success.
720 Journal of Applied Ecology. DOI: 10.1111/1365-2664.13605

721 26. Gandy, E.L., Yoch, D.C., 1988. relationship between nitrogen-fixing sulfate reducers and
722 fermenters in salt marsh sediments and roots of *Spartina alterniflora*. Applied and
723 Environmental Microbiology, 54:2031-2036.

724 27. Garcia-Robledo, E., Corzo, A., Papaspyrou, S., 2014. A fast and direct spectrophotometric
725 method for the sequential determination of nitrate and nitrite at low concentrations in small
726 volumes. Marine Chemistry, 162:30-36.

727 28. Gebrehiwet, T., Koretsky, C.M., Krishnamurthy, R.V., 2008. Influence of *Spartina* and
728 *Juncus* on saltmarsh sediments. III. Organic geochemistry. Chemical Geology, 255:114-
729 119.

730 29. Giurgevich, J.R., Dunn, E.L., 1979. Seasonal Patterns of CO_2 and Water Vapor Exchange
731 of the Tall and Short Height Forms of *Spartina alterniflora* Loisel in a Georgia Salt Marsh.
732 Oecologia, 43:139-156.

733 30. Gribsholt, B., Kostka, J. E., & Kristensen, E., 2003. Impact of fiddler crabs and plant roots
734 on sediment biogeochemistry in a Georgia saltmarsh. Marine Ecology Progress Series,
735 259:237-251.

736 31. Hassani, M.A., Durán, P., Hacquard, S., 2018. Microbial interactions within the plant
737 holobiont. Microbiome, 6:58.

738 32. Higashioka, Y., Kojima, H., Watanabe, M., Fukui, M., 2013. *Desulfatitalea tepidiphila*
739 gen. nov., sp. nov., a sulfate-reducing bacterium isolated from tidal flat sediment.
740 International journal of systematic and evolutionary microbiology, 63:761-765.

741 33. Higashioka, Y., Kojima, H., Watanabe, T., & Fukui, M., 2015. Draft genome sequence of
742 *Desulfatitalea tepidiphila* S28bFT. Genome announcements, 3(6), e01326-15.

743 34. Hong, Y., Liao, D., Hu, A., Wang, H., Chen, J., Khan, S., Su, J., Li, H., 2015. Diversity of
744 endophytic and rhizoplane bacterial communities associated with exotic *Spartina*
745 *alterniflora* and native mangrove using Illumina amplicon sequencing. Canadian journal
746 of microbiology, 61:723-733.

747 35. Hopkinson, C.S., Wolanski, E., Brinson, M.M., Cahoon, D.R., and Perillo, G.M.E., 2019.
748 Coastal Wetlands: A Synthesis. In: G.M.E., Perillo, E., Wolanski, D.R., Cahoon, and C.S.,
749 Hopkinson. (Eds.) Coastal Wetlands, Second Edition: An Integrated and Ecosystem
750 Approach. Elsevier, pp. 1–75.

751 36. Howarth, R.W., 1984. The ecological significance of sulfur in the energy dynamics of salt
752 marsh and coastal marine sediments. Biogeochemistry, 1:5-27.

753 37. Howes, B.L., Dacey, J.W.H., Goehringer, D.D., 1986. Factors controlling the growth
754 form of *Spartina alterniflora*: feedbacks between above-ground production, sediment
755 oxidation, nitrogen and salinity. Journal of Ecology, 74:881-898.

756 38. Hwang, Y-S., Morris, J.T., 1994. Whole-plant gas exchange responses of *Spartina*
757 *alterniflora* (Poaceae) to a range of constant and transient salinities. American Journal of
758 Botany, 81:659-665.

759 39. Hyun, J.H., Smith, A.C., Kostka, J.E., 2007. Relative contributions of sulfate-and iron (III)
760 reduction to organic matter mineralization and process controls in contrasting habitats of
761 the Georgia saltmarsh. Applied Geochemistry, 22:2637-2651.

762 40. Janssen, B., 1996. Nitrogen mineralization in relation to C:N ratio and decomposability of
763 organic materials. Plant Soil. 181:39–45

764 41. Joye, S.B., Hollibaugh, J.T., 1995. influence of sulfide inhibition of nitrification on
765 nitrogen regeneration in sediments. Science, 270:623-625.

766 42. Kembel, S., Cowan, P., Helmus, M., Cornwell, W., Morlon, H., Ackerly, D., Blomberg,
767 S., Webb, C., 2010. Picante: R tools for integrating phylogenies and ecology.
768 Bioinformatics, 26:1463–1464.
769 43. Kirwan, M.L., Guntenspergen, G.R., Morris, J.T., 2009. Latitudinal trends in *Spartina*
770 *alterniflora* productivity and the response of coastal marshes to global change. Global
771 Change Biology, 15:1982-1989.
772 44. Koch, M.S., Mendelssohn, I.A., McKee, K.L., 1990. Mechanism for the hydrogen
773 sulfide-induced growth limitation in wetland macrophytes. Limnology and
774 Oceanography, 35:399-408.

775 45. Kolton, M., Rolando, J.L., Kostka, J.E., 2020. Elucidation of the rhizosphere microbiome
776 linked to *Spartina alterniflora* phenotype in a salt marsh on Skidaway Island, Georgia,
777 USA. FEMS Microbiology Ecology, 96:fiaa026.

778 46. Koop-Jakobsen, K., Mueller, P., Meier, R.J., Liebsch, G., Jensen, K., 2018. Plant-sediment
779 interactions in salt marshes–an optode imaging study of O2, pH, and CO2 gradients in the
780 rhizosphere. Frontiers in plant science, 9:541.

781 47. Koretsky, C.M., Moore, C.M., Lowe, K.L., Meile, C., DiChristina, T.J., Van Cappellen, P.,
782 2003. Seasonal oscillation of microbial iron and sulfate reduction in saltmarsh sediments
783 (Sapelo Island, GA, USA). Biogeochemistry, 64:179-203.

784 48. Kostka, J.E., Gribsholt, B., Petrie, E., Dalton, D., Skelton, H.,Kristensen, E., 2002a. The
785 rates and pathways of carbon oxidation in bioturbated saltmarsh sediments. Limnology and
786 Oceanography, 47:230-240.

787 49. Kostka, J.E., Roychoudhury, A., Van Cappellen, P., 2002b. Rates and controls of anaerobic
788 microbial respiration across spatial and temporal gradients in saltmarsh sediments.
789 Biogeochemistry, 60:49-76.

790 50. Lee, R.W., Kraus, D.W., Doeller, J.E., 1999. Oxidation of sulfide by *Spartina alterniflora*
791 roots. Limnology and Oceanography, 44:1155-1159.

792 51. Lever, M.A., Torti, A., Eickenbusch, P., Michaud, A.B., Šantl-Temkiv, T., Jørgensen,
793 B.B., 2015. A modular method for the extraction of DNA and RNA, and the separation of
794 DNA pools from diverse environmental sample types. Frontiers in Microbiology, 6:476.

795 52. Lim, S.J., Davis, B.G., Gill, D.E., Walton, J., Nachman, E., Engel, A.S., Anderson, L.C.
796 and Campbell, B.J., 2019a. Taxonomic and functional heterogeneity of the gill microbiome
797 in a symbiotic coastal mangrove lucinid species. The ISME journal, 13:902-920.

53. Lim, S.J., Alexander, L., Engel, A.S., Paterson, A.T., Anderson, L.C., Campbell, B.J., 2019b. Extensive thioautotrophic gill endosymbiont diversity within a single *Ctena orbiculate* (Bivalvia: Lucinidae) population and implications for defining host-symbiont specificity and species recognition. mSystems, 4:e00280-19.

54. Lin, L., Liu, W., Zhang, M., Lin, X., Zhang, Y., Tian, Y., 2019. Different height forms of *Spartina alterniflora* might select their own rhizospheric bacterial communities in southern coast of China. Microbial Ecology, 77:124-135.

55. Liu, Y., Zhu, A., Tan, H., Cao, L., Zhang, R., 2019. Engineering banana endosphere microbiome to improve Fusarium wilt resistance in banana. Microbiome, 7:74.

56. Love, M.I., Huber, W., Anders, S., 2014. Moderated estimation of fold change and dispersion for RNA-seq data with DESeq2. Genome Biology, 15:550.

57. Lovell, C.R., Piceno, Y.M., Quattro, J.M., Bagwell, C.E., 2000. Molecular analysis of diazotroph diversity in the rhizosphere of the smooth cordgrass, *Spartina alterniflora*. Applied and Environmental Microbiology, 66:3814-3822.

58. Lundberg, D.S., Yourstone, S., Mieczkowski, P., Jones, C.D., Dangl, J.L., 2013. Practical innovations for high-throughput amplicon sequencing. Nature Methods, 10:999–1002.

59. Maricle, B.R., Lee, R.W., 2002. Aerenchyma development and oxygen transport in the estuarine cordgrasses Spartina alterniflora and S. anglica. Aquatic Botany, 74:109–120.

60. Martin, M., 2011. Cutadapt removes adapter sequences from high-throughput sequencing reads. EMBnet.Journal, 17:10-12.

61. Martin, B.C., Alarcon, M.S., Gleeson, D., Middleton, J.A., Fraser, M.W., Ryan, M.H., Holmer, M., Kendrick, G.A., Kilminster, K., 2020a. Root microbiomes as indicators of seagrass health. FEMS Microbiology Ecology, 96:fiz201.

62. Martin, B.C., Middleton, J.A., Fraser, M.W., Marshall, I.P., Scholz, V.V. and Schmidt, H., 2020b. Cutting out the middle clam: lucinid endosymbiotic bacteria are also associated with seagrass roots worldwide. The ISME journal, 14:2901-2905.

63. McMurdie, P.J., Holmes, S., 2013. phyloseq: an R package for reproducible interactive analysis and graphics of microbiome census data. PloS one, 8(4).

64. Mcowen, C.J., Weatherdon, L.V., Van Bochove, J.W., Sullivan, E., Blyth, S., Zockler, C., Stanwell-Smith, D., Kingston, N., Martin, C.S., Spalding, M., Fletcher, S., 2017. A global map of saltmarshes. Biodiversity data journal, 5: e11764.

65. Meier, D. V., Pjevac, P., Bach, W., Hourdez, S., Girguis, P. R., Vidoudez, C., et al., 2017. Niche partitioning of diverse sulfur-oxidizing bacteria at hydrothermal vents. The ISME Journal, 11:1545-1558.

66. Mendelssohn, I.A., 1979. the influence of nitrogen level, form, and application method on the growth response of *Spartina alterniflora* in North Carolina. Estuaries, 2:106-112.

834 67. Mendelssohn, I.A., McKee, K.L., 1992. Indicators of environmental stress in wetland
835 plants. In Ecological indicators (pp. 603-624). Springer, Boston, MA.

836 68. Mendelssohn, I.A., Morris, J.T., 2000. Eco-physiological controls on the productivity of
837 *Spartina alterniflora* Loisel. In: Weinstein, M.P., Kreeger, D.A. (Eds.). Concepts and
838 controversies in tidal marsh ecology. Kluwer Academic Publishers, pp. 59–80.

839 69. Mitsch, W. J., Gosselink, J. G., 1993. Wetlands. Van Nostrand Reinhold, New York, New
840 York, USA.

841 70. Morris, J.T., Dacey, J.W.H., 1984. Effects of O2 on ammonium uptake and root respiration
842 by *Spartina alterniflora*. American Journal of Botany, 71:979-985.

843 71. Morris, J.T., Haley, C., Krest, R., 1996. Effects of sulfide concentrations on growth and
844 dimethylsulphoniopropionate (DMSP) concentration in *Spartina alterniflora*. In: Kiene,
845 R., Visscher, R., Keller, M., Kirst, G. (Eds.) Biological and environmental chemistry of
846 DMSP and related sulfonium compounds. Plenum, pp. 87-95

847 72. Moulana, A., Anderson, R. E., Fortunato, C. S., Huber, J. A., 2020. Selection is a significant
848 driver of gene gain and loss in the pangenome of the bacterial genus *Sulfurovum* in
849 geographically distinct deep-sea hydrothermal vents. Msystems, 5:e00673-19.

850 73. Murphy, A.E., Bulseco, A.N., Ackerman, R., Vineis, J.H. and Bowen, J.L., 2020. Sulphide
851 addition favours respiratory ammonification (DNRA) over complete denitrification and
852 alters the active microbial community in salt marsh sediments. Environmental
853 Microbiology, 22:2124-2139.

854 74. Oksanen, J., Blanchet, F.G., Kindt, R., Legendre, P., Minchin, P.R., O'hara, R.B., Simpson,
855 G.L., Solymos, P., Stevens, M.H.H., Wagner, H., Oksanen, M.J., 2013. Package 'vegan'.
856 Community ecology package, version, 2(9), pp.1-295.

857 75. Petersen, J.M., Kemper, A., Gruber-Vodicka, H., Cardini, U., Van Der Geest, M., Kleiner,
858 M., Bulgheresi, S., Mußmann, M., Herbold, C., Seah, B.K., Antony, C.P., 2017.
859 Chemosynthetic symbionts of marine invertebrate animals are capable of nitrogen fixation.
860 Nature microbiology, 2:16195.

861 76. Peterson, B.J., 1999. Stable isotopes as tracers of organic matter input and transfer in
862 benthic food webs: A review. Acta Oecologica, 20:479-487.

863 77. Price, M.N., Dehal, P.S., Arkin, A.P., 2010. FastTree 2 – approximately maximum-
864 likelihood trees for large alignments. PLoS ONE, 5:e9490.

865 78. Quast, C., Pruesse, E., Yilmaz, P., Gerken, J., Schweer, T., Yarza, P., Peplies, J., Glöckner,
866 F.O., 2013. The SILVA ribosomal RNA gene database project: improved data processing
867 and web-based tools. Nucledic Acids Research, 41:D590-D596.

868 79. Ramírez, D.A., Yactayo, W., Rens, L.R., Rolando, J.L., Palacios, S., De Mendiburu, F.,
869 Mares, V., Barreda, C., Loayza, H., Monneveux, P., Zotarelli, L., Khan, A., Quiroz, R.,
870 2016. Defining biological thresholds associated to plant water status for monitoring water

restriction effects: Stomatal conductance and photosynthesis recovery as key indicators in potato. Agricultural Water Management, 177:369-378.

80. Ramnarine, R., Voroney, R.P., Wagner-Riddle, C., Dunfield, K.E., 2011. Carbonate removal by acid fumigation for measuring the $\delta^{13}C$ of soil organic carbon. Canadian Journal of Soil Science, 91:247–250.

81. Simmons, T., Caddell, D.F., Deng, S., Coleman-Derr, D., 2018. Exploring the root microbiome: extracting bacterial community data from the soil, rhizosphere, and root endosphere. Journal of Visualized Experiments, 135:e57561.

82. Schloss, P.D., Westcott, S.L., Ryabin, T., Hall, J.R., Hartmann, M., Hollister, E.B., Lesniewski, R.A., Oakley, B.B., Parks, D.H., Robinson, C.J., Sahl, J.W., 2009. Introducing mothur: open-source, platform-independent, community-supported software for describing and comparing microbial communities. Applied and Environmental Microbiology, 75:7537-7541.

83. Shade, A., Handelsman, J., 2012. Beyond the Venn diagram: the hunt for a core microbiome. Environmental microbiology, 14:4-12.

84. Sims, G.K., Ellsworth, T.R., Mulvaney, R.L., 1995. Microscale determination of inorganic nitrogen in water and soil extracts. Communications in Soil Science and Plant Analysis, 26:303–316.

85. Spivak, A.C., Reeve, J., 2015. Rapid cycling of recently fixed carbon in a *Spartina alterniflora* system: a stable isotope tracer experiment. Biogeochemistry 125:97-114.

86. Stegen, J.C., Lin, X., Konopka, A.E., Fredrickson, J.K., 2012. Stochastic and deterministic assembly processes in subsurface microbial communities. The ISME journal, 6:1653-1664.

87. Stegen, J.C., Lin, X., Fredrickson, J.K., Chen, X., Kennedy, D.W., Murray, C.J., Rockhold, M.L., Konopka, A., 2013. Quantifying community assembly processes and identifying features that impose them. The ISME journal, 7:2069-2079.

88. Stookey, L.L., 1970. Ferrozine - a new spectrophotometric reagent for iron. Anal. Chem. 43:779-781.

89. Suzuki, Y., Kojima, S., Sasaki, T., Suzuki, M., Utsumi, T., Watanabe, H., et al., 2006. Host-symbiont relationships in hydrothermal vent gastropods of the genus Alviniconcha from the Southwest Pacific. Applied and Environmental Microbiology, 72:1388-1393.

90. Suzuki, D., Li, Z., Cui, X., Zhang, C., Katayama, A., 2014. Reclassification of *Desulfobacterium anilini* as *Desulfatiglans anilini* comb. nov. within *Desulfatiglans* gen. nov., and description of a 4-chlorophenol-degrading sulfate-reducing bacterium, *Desulfatiglans parachlorophenolica* sp. nov. International journal of systematic and evolutionary microbiology, 64:3081-3086.

91. Thajudeen, J., Yousuf, J., Veetil, V. P., Varghese, S., Singh, A., Abdulla, M. H., 2017. Nitrogen fixing bacterial diversity in a tropical estuarine sediments. World Journal of Microbiology and Biotechnology, 33:41.

92. Thomas, F., Giblin, A.E., Cardon, Z.G., Sievert, S.M., 2014. Rhizosphere heterogeneity shapes abundance and activity of sulfur-oxidizing bacteria in vegetated salt marsh sediments. Frontiers in microbiology, 5:309.

93. Tobias C.R., Neubauer S.C., 2019. Salt marsh biogeochemistry—an overview. In: Perillo, G.M.E., Wolanski, E., Cahoon D.R., Brinson, M.M., (Eds.). Coastal wetlands: an integrated ecological approach. Elsevier, pp. 445–492.

94. Toju, H., Peay, K.G., Yamamichi, M., Narisawa, K., Hiruma, K., Naito, K., Fukuda, S., Ushio, M., Nakaoka, S., Onoda, Y., Yoshida, K., 2018. Core microbiomes for sustainable agroecosystems. Nature Plants, 4:247-257.

95. Trivedi, P., Leach, J. E., Tringe, S. G., Sa, T., Singh, B. K., 2020. Plant–microbiome interactions: from community assembly to plant health. Nature Reviews Microbiology, 18:607-621.

96. Valiela, I., Teal, J.M., Deuser, W.G., 1978. The nature of growth forms in the salt marsh grass *Spartina alterniflora*. The American Naturalist 112:461–470

97. Wang, Q., Garrity, G.M., Tiedje, J.M., Cole, J.R., 2007. Naive Bayesian classifier for rapid assignment of rRNA sequences into the new bacterial taxonomy. Applied and environmental microbiology, 73:5261–5267.

98. Watanabe, F.S., Olsen, S.R., 1965. Test of an ascorbic acid method for determining phosphorus in water and $NaHCO_3$ extracts from soil. Soil Science Society Proceedings, 29:677-678.

99. White, J.F., Kingsley, K.L., Zhang, Q., Verma, R., Obi, N., Dvinskikh, S., Elmore, M.T., Verma, S.K., Gond, S.K., Kowalski, K.P., 2019. Endophytic microbes and their potential applications in crop management. Pest management science, 75:2558-2565.

100. Whiting, G.J., Gandy, E.L., Yoch, D.C., 1986. Tight coupling of root-associated nitrogen fixation and plant photosynthesis in the salt marsh grass *Spartina alterniflora* and carbon dioxide enhancement of nitrogenase activity. Applied and Environmental Microbiology, 52:108-113.

101. Wieski, K., Pennings, S., 2014. Climate Drivers of *Spartina alterniflora* saltmarsh production in Georgia, USA. Ecosystems, 17:473-484.

102. Zhang, L., Zhang, W., Li, Q., Cui, R., Wang, Z., Wang, Y., Zhang, Y.Z., Ding, W., Shen, X., 2020. Deciphering the root endosphere microbiome of the desert plant *Alhagi sparsifolia* for drought resistance-promoting bacteria. Applied and Environmental Microbiology, 86:e02863-19.

103. Zheng, Y., Hou, L., Liu, M., Yin, G., Gao, J., Jiang, X., Lin, X., Li, X., Yu, C., Wang, R., 2016. Community composition and activity of anaerobic ammonium oxidation bacteria in the rhizosphere of salt-marsh grass *Spartina alterniflora*. Applied Microbiology and Biotechnology, 100:8203-8212.

946 104. Zogg, G.P., Travis, S.E., Brazeau, D.A., 2018. Strong associations between plant
947 genotypes and bacterial communities in a natural salt marsh. Ecology and Evolution
948 8:4721-4730.

949
950
951
952
953
954
955
956
957
958
959
960
961
962
963
964
965
966
967
968
969
970
971
972
973
974
975

Table 1: Analysis of the deterministic parameters controlling microbiome assembly. PERMANOVA analysis was conducted using the Bray-Curtis metric with 999 permutations. Results are provided for the complete data set and for microbiome compartments.

	All		Bulk sediment		Rhizosphere		Root	
Factor	F-value	R^2	F-value	R^2	F-value	R^2	F-value	R^2
Compartment	16.6	12.1**	-	-	-	-	-	-
S. alterniflora phenotype	12.0	8.8**	8.2	17.6**	7.1	16.1**	4.2	10.7**
Location	13.9	5.1**	9.2	9.8**	8.1	9.2**	4.7	5.9**
Depth	4.6	1.7**	3.2	3.5**	2.4	2.7**	2.7	3.4**
Year	2.3	0.8**	2.6	2.8**	1.5	1.7	1.6	2.0*

Figure 1: Statistical comparisons by linear regression analysis of average plant biomass and leaf natural ^{15}N abundance ($\delta^{15}N$) (a), sediment C:N ratio (b), sediment redox potential (Eh) (c), and leaf temperature (d). Plant biomass was calculated as the average of 10 individuals per sampling point. Each leaf $\delta^{15}N$, sediment C:N ratio, redox potential, and leaf temperature value represents the average of 3, 1, 3, and 5 replicates, respectively.

Figure 2: Statistical comparisons by linear regression analysis of enzyme activity rates and plant biomass assessed at Skidaway Island (a), and Sapelo Island (b). For each sample, rates were calculated from 8 time point measurements. Plant biomass represents the average of 10 individuals per sampling point.

Figure 3: Diversity and abundance of the *S. alterniflora* microbiome. Boxplots of the Shannon diversity index (a), and prokaryotic abundance determined by qPCR of SSU rRNA genes (b) per microbiome compartment and *S. alterniflora* phenotype. Evenness across plant compartments assessed by a cumulative rank-abundance plot (c). Non-metric multidimensional scaling (nMDS) ordination of the Bray-Curtis dissimilarity matrix across all collected samples with colors representing microbiome compartment (d) and *S. alterniflora* phenotype (e). nMDS stress: 0.10.

Figure 4: Relative abundance of putative nitrifiers (a), Fe oxidizers (b), S oxidizers (c), and S/sulfate reducers (d) by microbiome compartment and *S. alterniflora* phenotype.

Figure 5: Prokaryotic identity and relative abundance of the *S. alterniflora* rhizosphere and root core microbiome. Phylogenetic characterization was conducted using an approximately-maximum-likelihood model of the 72 ASVs comprising the *S. alterniflora* core rhizosphere and root microbiome. Taxonomic information at the genus level is provided for all ASVs. When taxonomic assignment was unknown at the genus level, the "Unk" prefix was used before the highest resolution taxonomic level assigned.

1035 **Figure 1:**

1036

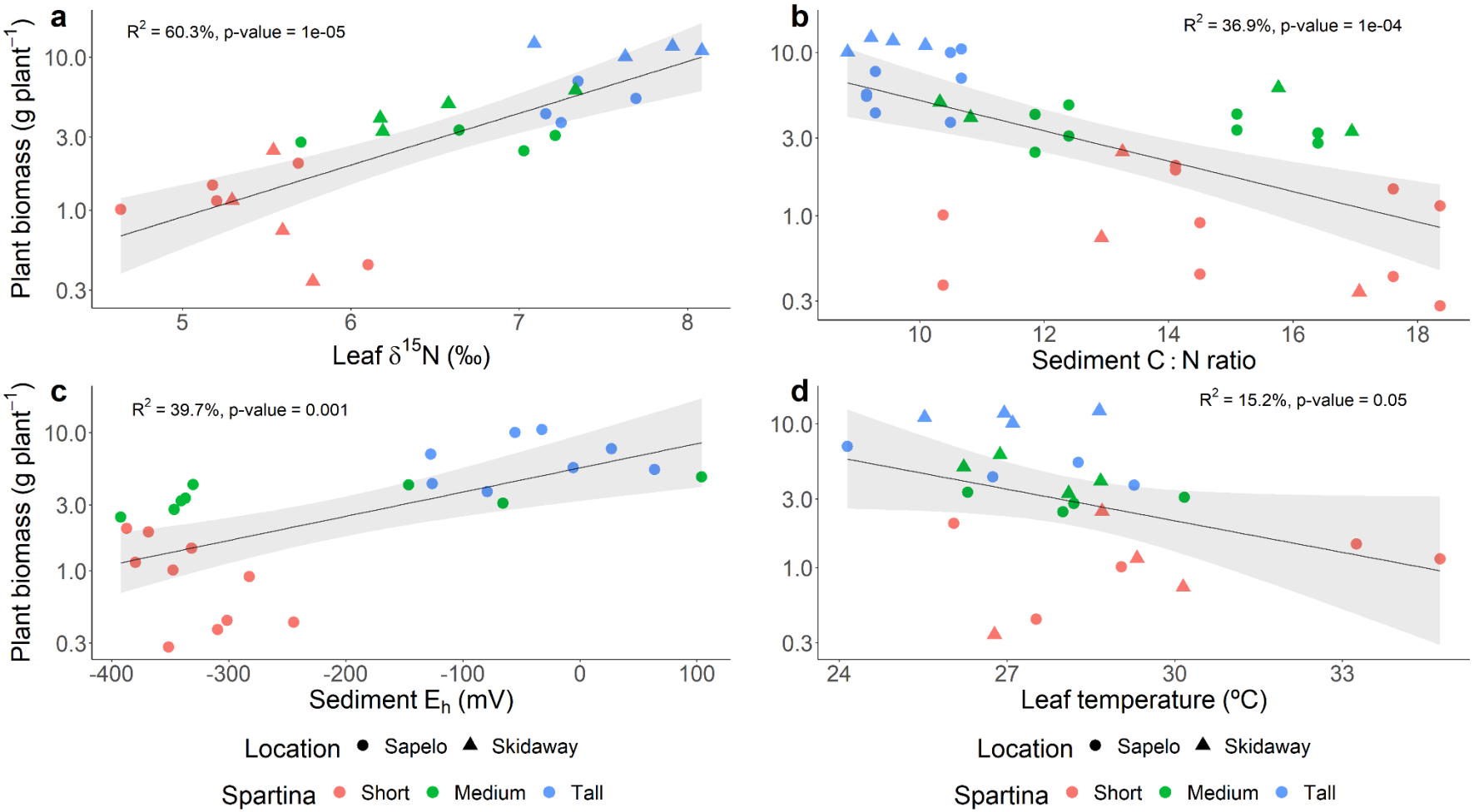

1037

1038

1039 **Figure 2:**

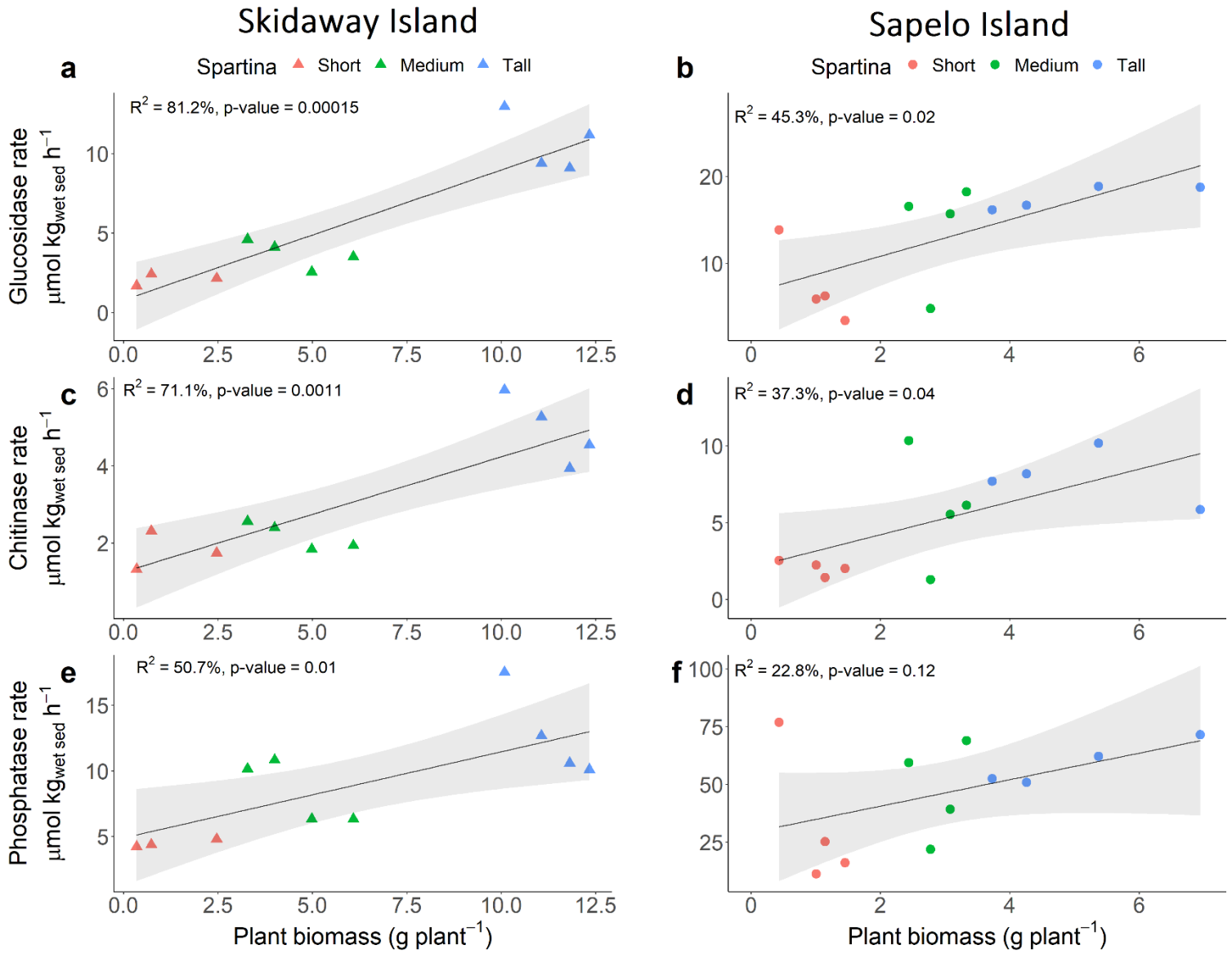

1040 **Figure 3:**

1041

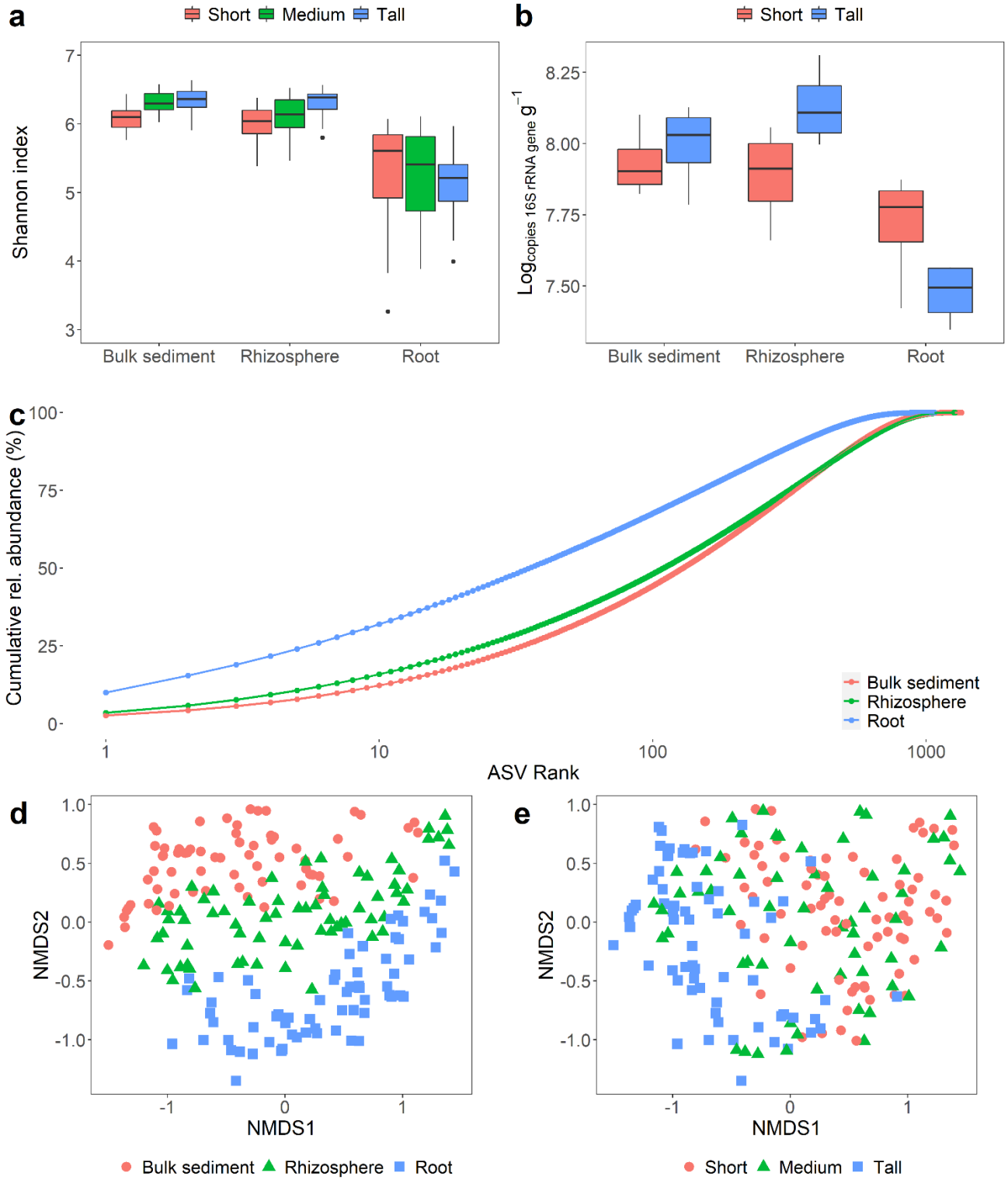

1042

1043 **Figure 4:**

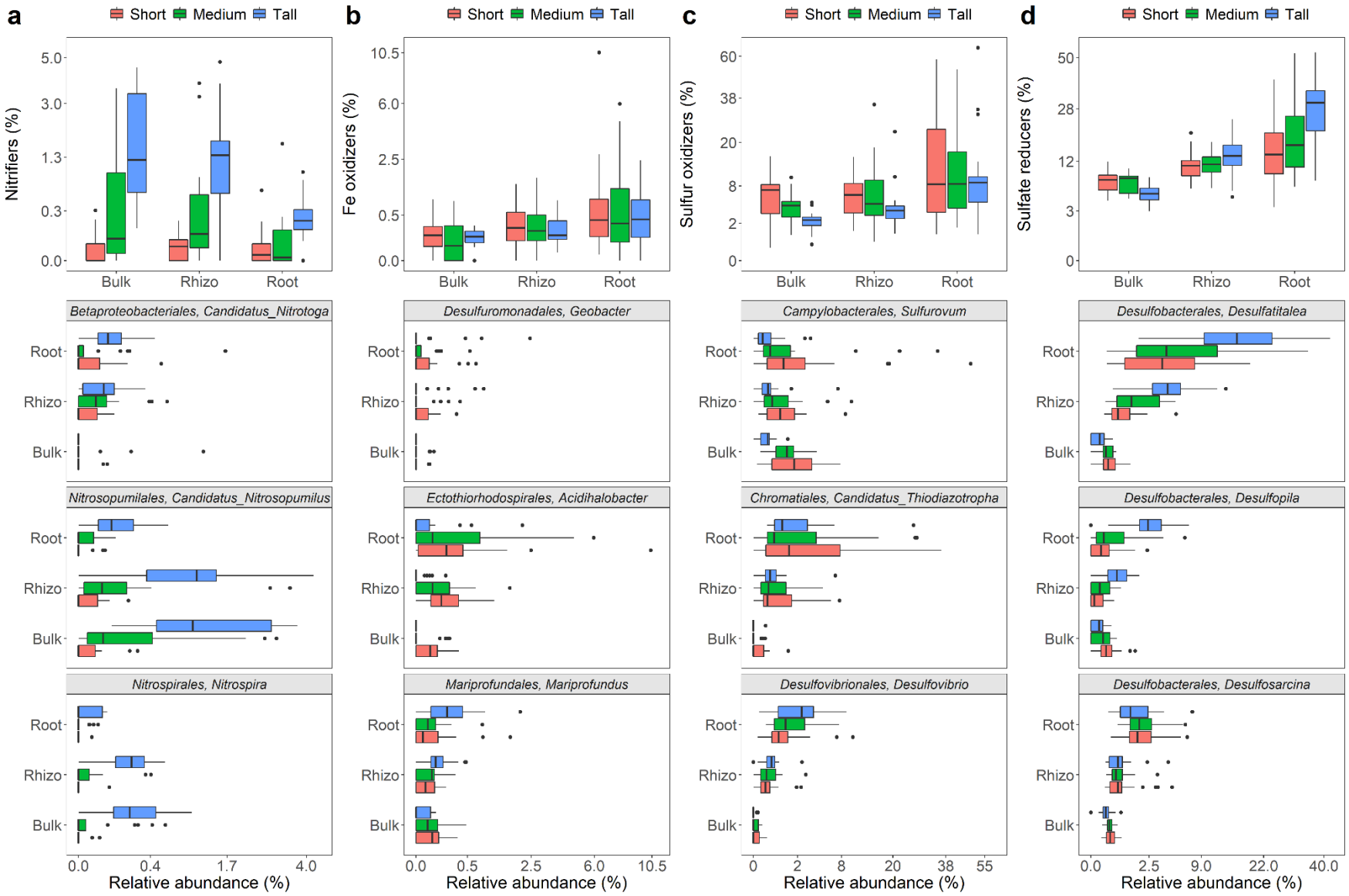

1044

1045 **Figure 5:**